Sensing the heat: the application of isothermal titration calorimetry to thermodynamic studies of biomolecular interactions

John E Ladbury[1] and Babur Z Chowdhry[2]

Biomolecular interactions can be defined by combining thermodynamic data on the energetic properties of the interaction with high-resolution structural data. The development of high sensitivity isothermal titration calorimetric equipment provides a dramatic advance in the gathering of thermodynamic data, and the interactions between biological macromolecules can now be described with unprecedented accuracy.

Addresses: [1]Department of Biochemistry, University College London, 91 Riding House Street, London, W1P 8BT, UK and [2]School of Biological and Chemical Sciences, University of Greenwich, Woolwich Campus, Wellington Street, London, SE18 6PF, UK.

Chemistry & Biology October 1996, **3**:791–801

Introduction

The study of how biological molecules interact with one another is fundamental to an understanding of the chemistry of life. A number of questions have to be addressed in these studies: how strong are the interactions? What defines the specificity of the interaction? What intermolecular interactions were present before a particular binding event, and how are they changed upon binding? The biological outcome of these interactions is dependent on a number of variables, such as the concentration of molecules present, the physical environment (including temperature, pressure and solvent) and the kinetics and thermodynamic consequences of the interaction. In the past, the thermodynamic parameters associated with biological interactions have been quantitated using methods such as spectroscopy; however, the recent development and commercial availability of instrumentation for high sensitivity isothermal titration calorimetry (ITC) has greatly enhanced our ability to measure these values directly and accurately. Here, we describe the ITC technique and discuss how the application of the fundamental physico-chemical data obtained by ITC may assist the design of novel biomimetic systems or lead to more efficient use of existing compounds.

The thermodynamics of interacting molecular species

The thermodynamics of interactions between different molecular species are determined by the number and types of bonds that are made by the component molecules. Thermodynamic measurements are usually concerned with equilibrium events, so reversibility of bond formation is requisite. In the transition from one defined state to another, hydrogen bonds, van der Waals (or London dispersion) interactions and hydrophobic interactions are formed or broken; it is the thermodynamic effect of these changes that is measured. Several events occur when two molecules interact to go from the free to the complexed state. In the free state, the molecules interact individually with solvent molecules. In an aqueous solvent, water will form hydrogen bonds with the exposed polar surfaces. In the vicinity of exposed apolar solute surfaces, water becomes organized, giving rise to a different hydrogen-bonding network than that among water molecules in the bulk solvent. The molecular degrees of freedom of water molecules are reduced in this more structured form compared to the more dynamic bulk solvent (see, for example, [1–3]). These noncovalent solvent associations are broken at the binding site, when interacting solute species come together and solvent molecules are

released. Concomitantly, the solute molecules form bonds and thus suffer restricted mobility. The change of interacting biomolecules from the free to the bound state thus produces a plethora of bonding rearrangements, which result in an overall change in the Gibbs energy of the system, $\Delta_B G^\circ$. This value has contributions from enthalpy ($\Delta_B H^\circ$) and entropy ($\Delta_B S^\circ$), and determining these parameters helps to characterize a given interaction. For example, the removal of water from an apolar surface, although requiring the enthalpically unfavourable destruction of hydrogen bonds between the solvent molecules, has a favourable entropic effect, resulting from the release of otherwise restricted water molecules into the bulk solvent. The balance of these effects differs from one interacting system to another; thus, each biomolecular interaction has a unique thermodynamic signature.

One of the primary goals in quantifying thermodynamic parameters of biological interactions (e.g., for formation of biopolymer–ligand complexes) is to elucidate how they relate to the structural effects of the interaction ([4] and references therein). Ultimately, knowledge of structural detail may permit the calculation of thermodynamic parameters of binding. There are numerous potential applications of such an understanding; one is in the pharmaceutical industry, where the affinities of potential drug compounds for a given binding site could be predicted, avoiding the temporally and financially expensive synthesis of these compounds and the need to perform binding studies with them. With the dramatic increase in the availability of high resolution structural detail and the use of ITC to determine the thermodynamic consequences of an interaction, the opportunity to approach this goal is apparent. Currently, the most fruitful approach has been to investigate the relationship between the temperature derivative of the components of Gibbs energy ($\Delta_B H^\circ$ and $\Delta_B S^\circ$), the change in heat capacity ($\Delta_B Cp$) and the surface area that is removed from exposure to solvent upon formation of a binding interaction [5–10]. A relationship between these parameters has been derived from studies of the heat of transfer of hydrocarbons into aqueous environments and of protein folding/unfolding equilibria, but the general principles should apply to any interacting species (see below).

ITC provides a direct route to the complete thermodynamic characterization of bimolecular equilibrium interactions. The molar calorimetric enthalpy and the equilibrium binding constant (K_B; this is equivalent to the reciprocal of the dissociation constant, K_d, commonly used in biochemistry) can be determined in one experiment by direct measurement of the heat of interaction as one component is titrated into the other (see below). The other thermodynamic parameters for the interaction are implicit from the relationship:

$$-R \bullet T \bullet \ln K_B = \Delta_B G^\circ = \Delta_B H^\circ - T\Delta_B S^\circ \qquad (1)$$

where R is the gas constant, T is the absolute experimental temperature and the other symbols are defined above. Modern instrumentation can determine K_B values in the range 10^3 to 10^9 M^{-1}. From experiments involving titration of the reactants, one may also directly determine the stoichiometry of the interaction from the molar ratio at the equivalence point. By performing titrations at a range of temperatures, the $\Delta_B Cp$ for an interaction can be determined from the following relationship:

$$\begin{aligned}\Delta_B Cp &= (\Delta_B H^\circ_{T2} - \Delta_B H^\circ_{T1}) / (T2 - T1) \\ &= (\Delta_B S^\circ_{T2} - \Delta_B S^\circ_{T1}) / \ln(T2 / T1)\end{aligned} \qquad (2)$$

where T1 and T2 are two temperatures at which independent experimental determinations have been made.

Calorimetric measurement is the only method available for directly determining the thermodynamic parameters associated with an interaction, since the enthalpy change provides the probe of the extent of an interaction. In other techniques (e.g., spectroscopic studies and equilibrium studies using isotopically labelled reactants) the binding constant can be determined, but the enthalpy has to be indirectly obtained from the van't Hoff relationship. Since discrepancies between the enthalpy values derived from calorimetric and van't Hoff methods have been observed, it is important that comparisons between data obtained directly and indirectly are done with caution [11]. Furthermore, other commonly used methods are based on the partitioning of two molecular components, requiring the respective amounts of free and bound material to be determined at a given concentration of one of the interacting components. Since this has to be done at a range of concentrations, these methods can be expensive in both time and material.

The ITC experiment

A schematic diagram of a standard ITC instrument is shown in Figure 1. The instrument consists of two identical cells (volume typically 0.5–1.5 ml) housed in an isothermal jacket. The jacket is cooled, so heat energy is required to keep the cells and their contents at the experimental temperature. These two cells are kept at thermal equilibrium ($\Delta T = 0$, see Fig. 1) throughout the experiment. One cell is filled with water (for experiments performed in aqueous solvents) or buffer solution, and acts purely as a reference. The other (the sample cell) is filled with one component of the interaction to be investigated. The basis of the experiment is to measure the heat energy per unit time (expressed in μW, although μcal s^{-1} is still used) that must be added to the sample cell to maintain zero temperature difference between the two cells at the designated temperature for an experiment. When the second component of the interaction is introduced in a series of aliquots (typically injections of 5–25 μl to give a total added volume of 50–250 μl) to the sample cell, an enthalpic change results.

Figure 1

A schematic diagram of a commercially available ITC instrument. The apparatus measures the heat energy per unit time that must be added to the sample cell to maintain zero temperature difference between the two cells at the designated temperature for an experiment.

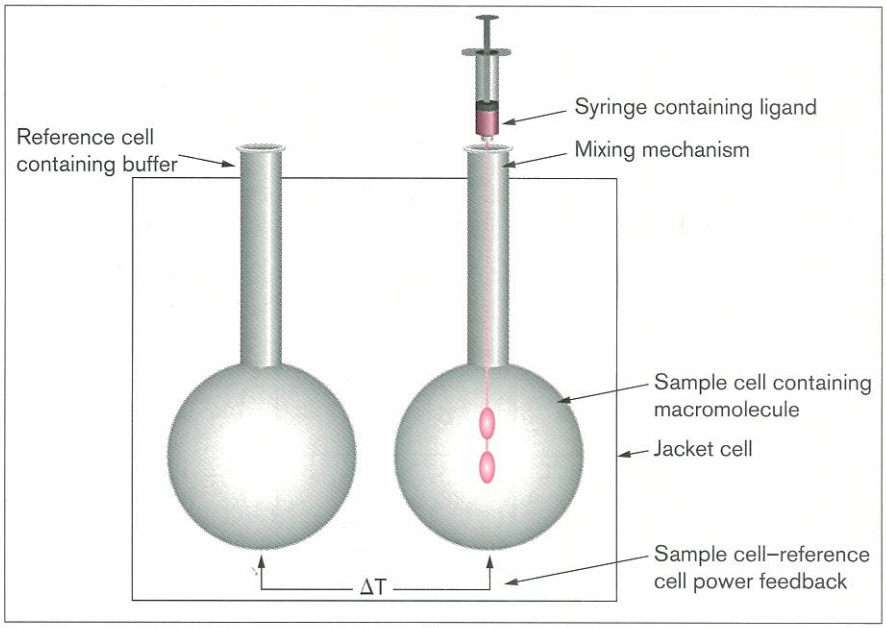

If the interaction is exothermic, less heat per unit time will be required by the sample cell to keep the two cells in thermal equilibrium; if the interaction is endothermic, the opposite effect will be observed. The cells are in contact with thermopile/thermocouple circuits regulated by an interactive feedback control system, so the highly sensitive response to fluctuations in temperature between the cells and between the jacket and the cells can be detected. Mixing of the interacting species, by stirring or by diffusion after fast injection, is very rapid and response times of instruments to incremental heats are typically less than 10 s. The high sensitivity of the instrument has resulted from vast improvements in the electronic components and the use of robust, thermally conducting materials for the calorimeter cells.

In an ideal experiment the concentrations of the two interacting molecular species are such that, over a series of additions, the available binding sites of the first reactant become saturated, so that the heat observed in the last few additions is solely due to the heat of dilution of the second component. A typical ITC experiment takes one to two hours, and an example of raw data output, plotted as the power output/input required to maintain the sample cell at the experimental temperature versus time, is shown in Figure 2a. The heat output per injection can be determined by integrating the peaks with respect to time; these data can be plotted against injection number or against the molar ratio of the components. The heats of dilution of both the reactants of the interaction are determined in separate titrations: adding the injectant into the cell containing buffer solution or adding buffer to the compound in the cell. The heats per injection for these two titrations are summed and subtracted from the raw data obtained in the initial experiment. For a 'simple' interaction, involving one independent site, the isothermal binding curve corrected for the heats of dilution has the sigmoidal form shown in Figure 2b.

The ITC experimental data output, represented graphically in Figure 2b, contains sufficient information to determine $\Delta_B H$, K_B, and the stoichiometry (n) of the interaction, if the initial concentrations of the interacting species are known [12–14]. Consider a 'simple' equilibrium interaction: $A + B \rightleftharpoons AB$, where A is in the calorimeter cell (of volume V) and B is added in equal volume aliquots. The fractional saturation, F, of species A at any point in the titration can be determined from the total heat output/input, Q, using the following equation:

$$Q = nFA_T\Delta_B HV \quad (3)$$

where A_T is the total concentration of A (free and complexed). Since $K_B = F/(1-F)[B]$ and $[B] = B_T - nFA_T$, the following quadratic relationship is obtained:

$$F2 - F\{1 + (B_T/nA_T) + (1/nK_BA_T)\} + (B_T/nA_T) = 0 \quad (4)$$

where B_T is the total concentration of B. Solving equation 4 for F and substituting this value into equation 3 gives:

$$Q = nA_T\Delta_B H\,(V/2) \bullet \{X - [X^2 - (4B_T/nA_T)]^{1/2}\} \quad (5)$$

where $X = \{1 + (B_T/nA_T) + (1/nK_BA_T)\}$. Thus, Q gives a value for the heat content of the interaction after a given

Figure 2

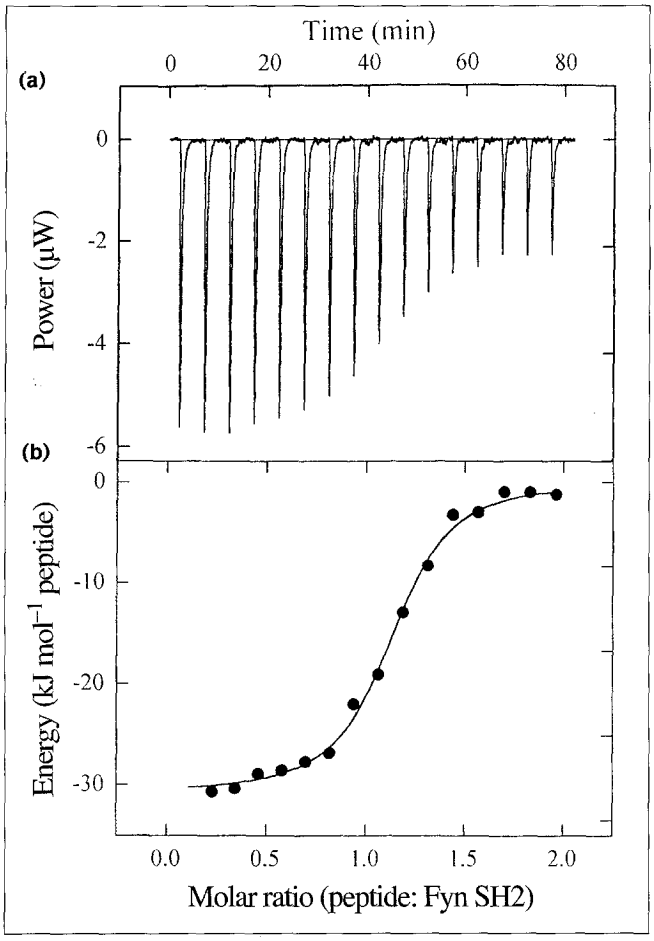

Sample ITC data. **(a)** Raw ITC data output for the exothermic interaction between a specific phosphotyrosyl peptide (210 μM) and the Fyn SH2 domain (21 μM) at 20 °C. **(b)** Titration plot derived from the integrated raw data from (a). The solid line represents the best least-squares fit to the data. The variable parameters are best fit by the following values: n = 1.09 (± 0.01), K_B = 2.42 (± 0.32) x 10^6 M, $\Delta_B H°$ = 30.88 (± 0.45) kJ mol^{-1}. The heat of dilution (17.56 kJ mol^{-1} injection^{-1}) was subtracted from the raw data prior to data analysis.

injection, which is dependent on the values of the independent variables $\Delta_B H$, K_B, and n. The values of the variables are obtained by fitting binding simulations for Q after each injection throughout the entire titration. In practice, this process involves an initial estimation of the variables, calculation of the change in Q for each injection based on these variables, and comparison of these values with the experimentally determined data. To improve the fit, Marquardt algorithms are used to reassign the values of the variables, based on the results of the previous step, and continued iterations are carried out until no further improvement of the fit occurs. These data are usually reported as a least-squares fit with inherent statistical error. From equation 5 above, it can be seen that the variation of K_B with A_T dictates the ultimate profile of the titration curve. Confidence in data fitting is highest when the product of these quantities is between 10 and 100, since outside this range, titration profiles have either too few data points in the region approaching equivalence or become linear, precluding appropriate fitting (see simulated binding isotherms in [13]). Therefore, for an interaction where we expect a value for K_B of about 10^6 M^{-1}, we require a concentration of A_T between 10 and 100 μM. The concentration of B required is calculated such that, for an interaction resulting in the formation of AB, the molar ratio of B to A at the end of the titration is two. Algorithms are available to fit binding data for more complex interactions, involving several independent or interactive binding events. These are beyond the scope of this review but are described elsewhere [12–14].

The precision with which temperature changes can be determined is obviously the ultimate limitation on the determination of power effects in ITC instrumentation. The differential temperature between the cells (ΔT) can typically be controlled to within 10^{-4} °C for the duration of an experiment. Changes of thermal power within the nanowatt range can be detected by the thermocouple junctions that are currently in use [13,14]. For small electrical pulses of 20 μJ, the standard error for 15 repeat determinations is ~1 μJ.

ITC has been applied to the study of a wide range of interactions, since the major requirement for determining the thermodynamic parameters of an interaction is that there is a measurable enthalpic effect. Here, we outline some of the areas where important recent advances have been made in our understanding of biomolecular interactions and describe where further investigations may take us (additional uses of ITC are given in Table 1). All the observed effects from the interactions described below are based on experiments carried out in aqueous solvents and thus are more relevant to physiological conditions than are other studies performed in nonaqueous environments.

Determinants of the stability of biomolecular interactions

The stability of protein structure

Selective cleavage of ribonuclease A (RNase A) by subtilisin produces a 20-residue peptide (S-peptide) and a 104-residue fragment (S-protein). The interaction of S-protein with S-peptide has provided a valuable model for studying the thermodynamics of protein–peptide interactions and ligand binding in general [15–17]. The two cleavage products interact with each other to produce a complex (RNase S), which has some nuclease activity. Since residues 16–20 of S-peptide are essentially unstructured in RNase A and do not appear to interact with the S-protein in RNase S, most binding studies have used peptides containing residues 1–15.

Table 1

Applications of ITC.

Higher order nucleic acid structure formation
Interaction of protein domains with macromolecules and ligands
Protein–protein, protein–peptide, protein–ligand, nucleic acid–ligand (e.g., drug), protein–nucleic acid interactions
pH and solvent induced changes in macromolecules
Metal-ion binding to molecules
Structural assembly and functional regulation of molecules
Receptor–ligand interactions
Ligand-induced oligomerization
Effects of cosolvents and denaturants
Role of water in biological systems
Enthalpy of transfer of molecules from aqueous phase to nonaqueous or lipid phases
Reactant concentration effects
Hormone–receptor interactions
Antibody–antigen interactions
Enzyme–substrate/cofactor/substrate analogue interactions
Interactions between components of multimolecular complexes including membrane proteins and multisubunit enzymes
Carbohydrate binding to other macromolecules
Cell–ligand interactions
Metal/ligand/macromolecule–model membrane interactions
Effect of chemical modification of ligands on macromolecule–ligand interaction
ΔH for protonation/deprotonation of molecules

Several studies on the thermodynamics of binding of S-peptide to S-protein have been performed using S-peptides with altered amino-acid sequences. Examination of the thermodynamic effects of amino-acid substitutions in peptides has some advantages over the more widely used methods based on denaturation/renaturation of proteins with site-specific amino-acid mutations. The production of short defined peptides is far easier than the laborious task of recombinant DNA manipulation, expression and purification of a mutant protein. Also, denaturation studies require that the comparison between a wild-type and mutant protein is based on a common defined state (the denatured state). It is becoming clear, however, that in many cases the denatured state of a protein can have some structure, which can be affected by the amino-acid composition. Thus, it cannot be assumed that the denatured state will be equivalent for wild-type and mutant proteins. In addition, problems with data interpretation can arise from the method of denaturation; for chemical denaturation, the equilibria for the interaction of proteins with the denaturants are not fully understood, and for heat denaturation the additional effects of heats of ionization of buffer solutions have to be taken into account.

ITC studies were performed on S-protein binding to seven forms of S-peptide in which the methionine at position 13 (Met13) had been substituted by different amino acids. Crystallographic data indicated that Met13 has an important role in the formation of RNase S, because it buries into the hydrophobic core of the protein upon binding. The binding of all the mutant S-peptides to S-protein was of lower affinity than that of the wild-type peptide [15–17]. At pH 6.0 and 25 °C, $\Delta\Delta_BG^\circ$ values for the Met13→Ile and Met13→Gly substitutions were 0.8 and 21 kJ mol^{-1} respectively ($\Delta\Delta_BG^\circ = \Delta_BG^\circ_{(\text{mutant peptide})} - \Delta_BG^\circ_{(\text{wild-type peptide})}$). These Gibbs energy values can be reconciled by the structural changes that occur in the S-peptides on binding to the S-protein. The structure of an isoleucine sidechain has some similarity to that of a methionine sidechain, and both have hydrophobic character. Thus the methionine to isoleucine substitution is conservative, and the $\Delta\Delta_BG^\circ$ of the Met13→Ile peptide is low. On the other hand the glycine sidechain consists solely of a hydrogen atom; thus, this residue in the unbound peptide has far fewer steric structural restraints (can adopt many more ϕ and ψ angles) than the wild-type methionine. On binding to the S-protein, the structure of the Met13→Gly peptide is much more restricted than that of the wild-type peptide. This effect is demonstrated by the fact that the $\Delta\Delta_BS^\circ$ for the Met13→Gly, compared to wild-type, is much more unfavourable (more negative) than for any of the other mutant peptides. Δ_BCp was determined by measuring the thermodynamic parameters for the binding of S-peptide, and several substituted peptides, to S-protein over a range of temperatures [16]. In all cases, no relationship was observed between Δ_BCp and the surface area buried upon binding. The reason for this is not clear, although the tolerance of this relationship may only hold for large molecular systems rather than for single amino-acid substitutions.

The stability of complex nucleic acid structures

The thermodynamic parameters associated with the equilibrium association of oligonucleotides have not been widely investigated by ITC methodology. There is certainly scope for these types of studies by calorimetry, although the problems of unspecified structural effects such as fraying (the incomplete binding of single strands throughout the length of a duplex) and super-structural formation make such studies intellectually challenging.

There is, however, increasing interest in this field. Short oligonucleotides can bind to a DNA duplex, forming a triple helix. Oligonucleotides can thus be used to selectively recognize sequences of double-stranded DNA and may prove useful in this capacity as therapeutic agents to block expression of aberrant genes. We thus expect a large increase in the acquisition of thermodynamic information on these systems.

ITC studies have been performed on the formation of complex DNA structures corresponding to the intersection points of single-stranded oligonucleotides, such as Holliday four-armed junctions [18] and three-way junctions (TWJs) [19]. The arms of these structures are duplex DNA and each component single strand is involved in forming two arms. This gives rise to a junction point where the single strands cross each other, and which may form a recognition site for interactions with proteins or ribozymes. The multi-component nature of these interactions requires either a reductionist approach to thermodynamic characterization (which involves the measurement of the individual bimolecular strand interactions in isolation [18]); or the measurement of the effect of adding a third component to a previously characterized bimolecular interaction [19]. In the latter strategy, the thermodynamic properties of one interaction must be substantially different from the other, so as not to interfere.

The sum of the Gibbs energies of formation of the individual arms of a TWJ was found to be ~25 kJ mol^{-1} less than the Gibbs energy for the formation of the TWJ itself. This indicated that the insertion of a junction into duplex oligonucleotides is a thermodynamically unfavourable process. The interaction of oligonucleotides in these structures is characterized by a large negative $\Delta_B Cp$ per base pair (e.g., values of –259 J mol^{-1} K^{-1} [18] and –364 J mol^{-1} K^{-1} [19] have been obtained). This may be consistent with the removal of a large surface area of the molecule from exposure to solvent. The limited structural information available on oligonucleotides indicates, however, that the extent of hydration is important for their stability [20]; thus, it may be necessary to consider the role of water when determining the change in heat capacity (see below).

Enthalpy and entropy of drug–DNA interactions

The study of the binding of low molecular weight ligands to DNA is an area of intense interest in many laboratories. Such investigations are motivated by the need to develop more specific and less toxic therapeutic agents and by a fundamental interest in the physico-chemical and structural properties of the DNA molecule.

Interactions of drugs with DNA are often characterized by small enthalpic changes, and the contributions of these changes to free energy have been measured by high sensitivity ITC techniques. For example, the Δ and Λ isomers of $[Ru(phen)_2DPPZ]^{2+}$ form part of a family of ruthenium(II) complexes containing planar aromatic ligands, which have been extensively studied because of their suitability as probes of DNA structure. ITC has been used to determine directly the $\Delta_B H^\circ$ at 25 °C for the interaction of the two isomers with calf thymus DNA [21]. These experiments were designed such that the quantity of DNA in the sample cell was always in excess, ensuring that all of the added titrant (ligand) would bind. $\Delta_B H^\circ$ values were determined to be +0.8 kJ mol^{-1} for the Δ isomer and +12.1 kJ mol^{-1} for the Λ isomer. The small size and positive sign of these enthalpy values were qualitatively confirmed indirectly using the van't Hoff relationship from data obtained from UV thermal-difference spectroscopy. These data clearly indicated that the binding of these ligands to DNA is entropically driven. This is unusual, since ITC studies of other DNA intercalants, including ethidium [22] and daunomycin [23], indicate the binding of these drugs to DNA is enthalpically driven. $[Ru(phen)_2DPPZ]^{2+}$ comprises an intercalating chromophore to which two hydrophobic phenanthroline side groups are attached. It seems that fitting these bulky side groups into the DNA minor groove may result in a large entropically favourable effect, presumably from the release of water from the binding interface. This study elegantly showed how ITC can be used to solve difficult problems in the study of nucleic acid–drug interactions.

The specificity of biomolecular interactions

Specificity in protein-mediated intracellular signalling

ITC has been used to address several important questions in the study of protein–protein interactions. In many cases polypeptides and short peptide sequences have been used as models to represent these interactions. It is wrong, however, to assume that the thermodynamic properties of an interaction involving a peptide are necessarily equivalent to those involving a whole protein. Often the small size of peptides precludes formation of the native folds found in whole proteins. There will thus be a free energy cost involved in producing the recognized structural context for binding in the peptide. This should be borne in mind when interpreting data obtained using model peptides.

ITC studies have been invaluable in understanding the specificity of proteins involved in intracellular signal transduction. For example, several signalling pathways involve the interaction of proteins containing Src homology 2 (SH2) domains with proteins containing phosphorylated tyrosine residues. SH2 domains are found in a large number of cytoplasmic proteins. They consist of approximately 100 amino-acid residues and have a high level of similarity in sequence and secondary structure. A plethora of reactions are mediated by the interaction of phosphorylated tyrosine residues and SH2 domains, some of which are apparent in the same signalling pathway. The importance of the integrity of these pathways is demonstrated by the fact that mutations that give rise to a loss of function in these SH2

domains can cause cellular transformation, leading to tumor formation, immunodeficiency or metabolic disorders. Since all of the SH2 domains examined thus far have great similarity in their secondary structure, it is an intriguing problem to decipher what determines the specificity of their interactions, preventing 'crossed lines'.

Some of the subtle differences between the thermodynamic consequences of the interactions between selected SH2 domains and specific and nonspecific tyrosyl phosphopeptides have been determined using ITC analysis. [24–26]. Perhaps the most striking observation is that, for all of the interactions, the enthalpic term is the overwhelmingly dominant contribution to the Gibbs energy of interaction over a range of temperatures, including 25 °C (Table 2a). The net entropy change on binding is negligible, indicating that any positive entropic contribution derived from the liberation of water molecules into bulk solvent is compensated by conformational changes in the SH2 domain or the tyrosyl phosphopeptide. When the interactions of the Src or Fyn SH2 domains with their specific peptides are compared to that of the Lck SH2 domain with a nonspecific peptide at 25 °C, there is less than an order of magnitude difference between the binding affinities. Assuming that these SH2–peptide interactions are physiologically relevant, there seems to be little specificity involved; indeed it would seem that an increase in the effective concentration of the nonspecific peptide could easily result in signalling errors. This is potentially difficult to understand, unless one invokes other mechanisms for providing specificity in signal transduction, for example, the parallel processing of signals and/or the temporal effects of binding interactions, such that on and off rates in parallel signalling processes will add a further element of specificity.

The interaction of SH2 domains with tyrosyl phosphopeptides can also be used to demonstrate how structural data can be complemented by thermodynamic measurement. Table 2b shows the thermodynamic data for the interaction of the Fyn SH2 domain with a specific or a nonspecific phosphotyrosyl peptide at 30 °C. At this temperature, NMR spectral data indicated that, whereas the specific peptide appeared to interact with the SH2 domain through several amino-acid residues, the nonspecific peptide was mobile in regions distal from the phosphotyrosine residue [27]. This structural phenomenon is apparently reflected in the thermodynamic data; although there is a reduced Gibbs energy of binding for the nonspecific peptide, the entropic term is actually increased over that of the specific peptide. This is consistent with a less restricted bound state.

Specific and nonspecific protein–DNA interactions

The thermodynamic characterization of protein–DNA interactions is of great importance in understanding gene regulation and transcription [28]. Proteins interact with DNA in at least two distinct ways: in a specific interaction the protein binds to a certain sequence of nucleotides, which form a cognate site; in a nonspecific interaction the protein binds to DNA but does not recognize a given sequence. Specific protein–DNA interactions are typically high-affinity, often outside the useful range of current ITC instrumentation. However, calorimetric methods for the characterization of tight binding have been explored [29,30]. As described above, the determination of $\Delta_B Cp$ for interactions is important for relating thermodynamics to structural detail. This parameter can be determined without fitting the titration data for the binding constant. The exposed surface of DNA shows little structural definition and thus presents many potential binding sites to a protein for nonspecific interactions; yet proteins are able to bind to DNA very specifically and with high affinity. It has been proposed that nonspecific interactions are physiologically important for localizing the protein to the DNA, restricting the search for the cognate site to one dimension [31]. ITC data indicate that the difference in Gibbs energy for specific versus nonspecific interactions is typically greater than 8 kJ mol^{-1} [32,33].

Specific interactions of protein with DNA are generally accompanied by a large negative $\Delta_B Cp$, for example, for the interaction of the *trp* repressor protein dimer with an oligonucleotide corresponding to the *trp* repressor binding site, *trp* operator, $\Delta_B Cp = -3.97$ kJ mol^{-1} K^{-1} [32], and for the interaction of MetJ repressor protein dimer with an oligonucleotide corresponding to the operator known as the metbox, $\Delta_B Cp = -2.42$ kJ mol^{-1} K^{-1} [33]. In contrast, nonspecific protein–DNA interactions have little or no associated $\Delta_B Cp$. Since there seems to be some relationship between the $\Delta_B Cp$ and the burial of surface area (as mentioned above), these data may indicate that the thermodynamic consequence of a specific interaction is the removal of some or all of the solvent from the interactive interface, whereas solvent still has a key role in the nonspecific interaction. This is an appealing hypothesis, since it has been demonstrated that nonspecific interactions are largely due to electrostatic effects (rather than to direct hydrogen or van der Waals interactions) which do not preclude the involvement of molecules with high dielectric constants such as water.

The stoichiometry of biomolecular interactions

The stoichiometry of protein–DNA interactions

The stoichiometry of an interaction can be determined by ITC from the molar ratio of interacting species at the equivalence point (assuming that the concentration of both of the interacting species is known). This has been demonstrated for the interaction of *trp* repressor with a 20-base-pair oligonucleotide containing the operator site (Fig. 3a) [32]. The repressor molecule recognizes a palindromic duplex DNA sequence, forming a specific primary binding interaction. However, the oligonucleotide sequence used in this study contains a sequence corresponding to half of

Table 2

(a) Thermodynamic parameters determined for the binding of SH2 domains to tyrosyl phosphopeptides at 25 °C.

	$K_B \times 10^{-6}$ M^{-1}	$\Delta_B G°$ kJ mol^{-1}	$\Delta_B H°$ kJ mol^{-1}	$T\Delta_B S°$ kJ mol^{-1}	$\Delta_B S°$ J mol^{-1} K^{-1}
Src SH2 domain–specific peptide (pYEEI motif)*	1.63	−35.41	−35.28	+0.13	+0.43
Fyn SH2 domain–specific peptide (pYEEI motif)†	1.36	−35.00	−35.61	−0.61	−0.02
p85 SH2 domain–specific peptide (pY751 from PDGFR)*	2.30	−36.24	−39.25	−3.01	−10.10
Lck SH2 domain–nonspecific peptide (pY505 from Lck C-terminus)*	0.32	−31.35	−31.46	−0.11	−0.37

(b) Thermodynamic parameters determined for the binding of the Fyn SH2 domain to tyrosyl phosphopeptides at 30 °C.

	$K_B \times 10^{-6}$ M^{-1}	$\Delta_B G°$ kJ mol^{-1}	$\Delta_B H°$ kJ mol^{-1}	$T\Delta_B S°$ kJ mol^{-1}	$\Delta_B S°$ J mol^{-1} K^{-1}
Fyn SH2 domain–specific peptide (pYEEI motif)†	0.70	−33.91	−42.20	−8.29	−27.35
Fyn SH2 domain–nonspecific peptide (pY531 from Fyn C-terminus)†	0.02	−24.96	−20.21	+4.75	+15.67

*Values taken from [26]

†Values taken from [27]

the palindrome, which could result in a secondary interaction. ITC experiments on *trp* repressor–operator interactions confirmed that both binding events occurred. At 13 °C, unusual, nonsigmoidal binding isotherm profiles were obtained (Fig. 3b), which could be fit by a model in which an initial tight exothermic binding occurs with a stoichiometry of one repressor dimer per oligonucleotide molecule ($K_B \approx 10^9\ M^{-1}$; $\Delta_B H° = -27$ kJ mol^{-1}). When more of the repressor molecule is added, this initial binding event becomes saturated, and a second, weaker endothermic binding event occurs, correspon-ding to the half-site interaction ($K_B = 2.2 \times 10^5\ M^{-1}$; $\Delta_B H° = +46$ kJ mol^{-1}). Once this secondary site becomes saturated no further heat of binding is observed. This sequential binding effect would not have been discernible by many other techniques.

The stoichiometry of receptor–growth factor interactions

The mechanism of signal transduction through a cell membrane upon the interaction of a receptor with a stimulating ligand (e.g., a growth factor, a hormone or a cytokine) is still not fully understood. In many cases the binding of a ligand results in oligomerization of receptor molecules. It is this association that is believed to transmit a signal through the membrane. ITC has been used to explore the interaction of molecules in receptor systems to elucidate the stoichiometry and thermodynamic parameters of the interaction.

Human growth hormone (hGH) interacts with two molecules of the hGH receptor, indicating that this divalent ligand is involved in bringing receptor molecules together to initiate a signalling process [34]. This is similar to the initial interaction of epidermal growth factor (EGF) with its receptor molecule. In this system, ITC experiments suggested a stoichiometry of one EGF molecule bound to two EGF receptor molecules (J.E.L. and M.A. Lemmon, unpublished data). The ITC data indicated that the thermodynamic parameters associated with the binding of EGF to the individual receptor molecules in the complex were distinct. When more EGF was added to the solution containing ligand–receptor complexes, an additional binding event was observed, suggesting that the growth factor–receptor complex can accommodate two divalent ligands.

The mode of binding of the acidic fibroblast growth factor (aFGF) to its receptor has also been investigated by ITC [35]. aFGF clearly forms a 1:1 complex with its receptor; however, an accessory molecule, heparan sulfate, is also involved in the binding. This polysaccharide is found in the extracellular matrix adjacent to cell surfaces; it binds to aFGF, localizing it to the cell surface and arranging the monovalent growth-factor ligands so they can bind as dimers that bring two receptors together. The formation of the dimeric ligand–receptor complex in the presence of heparan sulfate was clearly demonstrated using ITC [35].

Surface-area burial and the change in heat capacity

Burial of hydrophobic surface

Deciphering the relationship between changes in thermodynamic parameters and the structural features of the molecules contributing to an interaction is of fundamental importance for understanding the forces that drive biological processes under equilibrium conditions. The first insight into these forces comes from the connection between $\Delta_B Cp$ and the burial of surface area on the interacting molecules. The contribution to $\Delta_B Cp$ from the burial of hydrophobic surface is dominant over that from burial of hydrophilic surface. Several groups have developed algorithms relating $\Delta_B Cp$ to burial of apolar surfaces; these

Figure 3

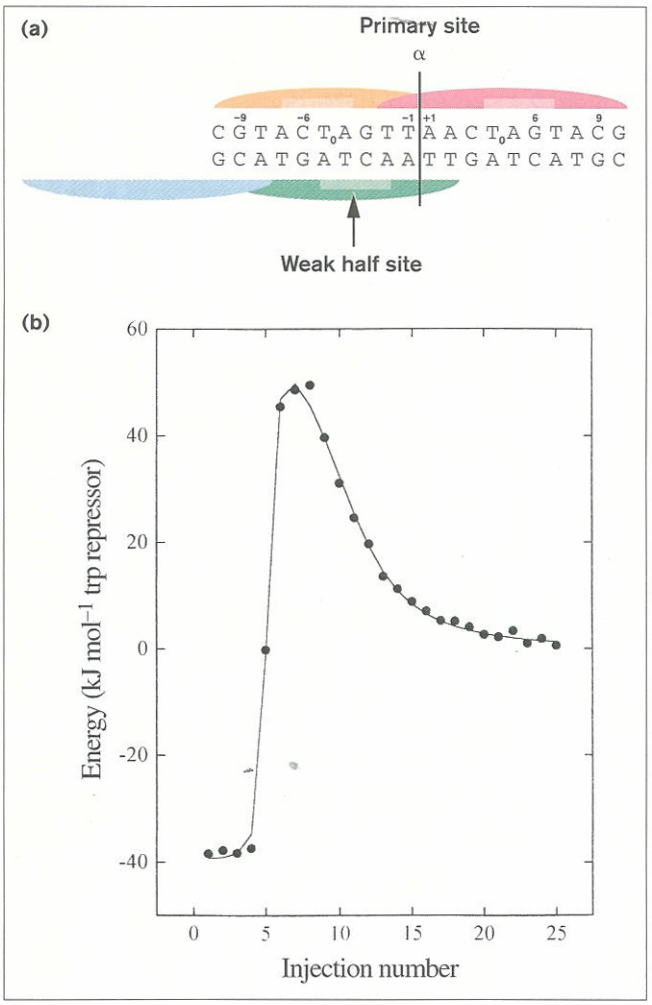

ITC data on the binding of *trp* repressor to its operator sequence reveals a second binding event to a half site at high repressor concentration. **(a)** A schematic diagram depicting the interaction of the *trp* repressor dimer with a 20-base-pair oligonucleotide incorporating the cognate operator site. The oligonucleotide has the potential to form a primary interaction binding site at the palindromic sequence as well as a secondary half-site for repressor binding. **(b)** ITC data for the interaction of *trp* repressor dimer (615 mM) with a 20-base-pair oligonucleotide incorporating the cognate operator site (42.1 mM). The solid line is the result of a least-squares fit for two independent binding events [32].

studies indicate that the average contribution to $\Delta_B Cp$ from apolar surface burial is ~1.67 ± 0.17 J mol^{-1} K^{-1} Å^{-2} [7,8,10]. Although the contribution is smaller, recent algorithms relating $\Delta_B Cp$ to surface-area burial have also included contributions from polar moieties (see, for example, [36]). As pointed out by Sturtevant, however, there are several other potential sources of heat capacity change that could also be important [5] (see below).

ITC data for the high-affinity interaction of the immunosuppressive agent FK506 with the protein FKBP-12 also supported the existence of a relationship between $\Delta_B Cp$ and surface-area burial (calculated $\Delta_B Cp$ = –1.04 kJ mol^{-1} K^{-1}; experimental $\Delta_B Cp$ = –1.09 kJ mol^{-1} K^{-1}) [37]. The interactive surface between these two molecules is almost entirely hydrophobic; thus, the interdependence of $\Delta_B Cp$ and apolar surface area could be refined to specify contributions from aromatic and aliphatic hydrophobic groups to give the equation:

$$\Delta_B Cp_{nonpolar} = 1.13\ \Delta_B A_{aromatic} + 1.68\ \Delta_B A_{nonaromatic}$$

where the change in heat capacity is measured in J mol^{-1} K^{-1} Å^{-2}.

The role of water in biomolecular interactions

The relationship between $\Delta_B Cp$ and surface-area burial does not apply in all cases. For example, the interaction between *trp* repressor and a 20-base-pair oligonucleotide containing its cognate operator site gave a $\Delta_B Cp$ calculated from ITC data that was less than half that of the experimentally determined value (calculated –1.8 kJ mol^{-1} K^{-1}, experimental –4.0 kJ mol^{-1} K^{-1}) [32]. This lack of correlation with the derived relationship is also observed in the case of MetJ binding to an oligonucleotide corresponding to the metbox sequence [33,38]. How can these differences be resolved? On closer examination of the X-ray crystallographic data for these protein–DNA complexes, it is apparent that there are several water molecules present in the binding site (Fig. 4). For the *trp* repressor, X-ray crystallographic structures have been solved for both the unbound and complexed components to better than 2 Å resolution, and several water molecules form hydrogen bonds between the protein and DNA. Indeed, the use of mutant proteins or DNA analogues that preclude the formation of these hydrogen bonds reduces the affinity of the interaction. On the basis of these observations it has been suggested that there is an additional contribution to the heat capacity of the complexed form derived from the restriction of water molecules in the interface between interacting molecules, probably as a result of reduction in soft vibrational modes (as previously predicted) [5]. Thus, the formation of specific interactions by water molecules at a biomolecular interface may actually increase the binding affinity, because increasing $\Delta_B Cp$ can result in increased $\Delta_B G^\circ$ at a given temperature. Designing drug molecules that are able to incorporate hydrogen-bonding water molecules into the interface with a target molecule may result in improved efficacy.

Conclusions

The complete thermodynamic parameters of an interaction can be characterized by direct measurement of the enthalpy at equilibrium conditions over the course of a titration. This information has provided insights into the stability, specificity, and stoichiometry of numerous

Figure 4

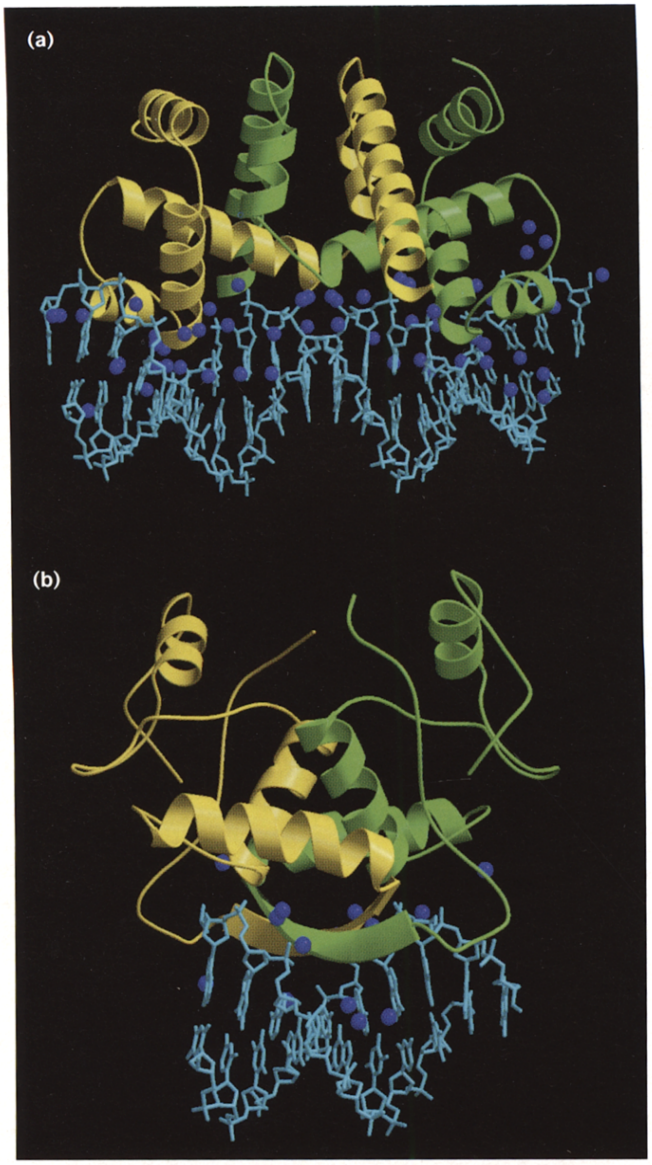

The X-ray crystal structures of the *trp* repressor–operator complex and the MetJ–metbox complex reveal that water molecules are present in the binding site. Only water molecules that are positioned within 3.0 Å of both the protein and DNA are shown. For clarity, the co-factor molecules have been removed. **(a)** Representation of the X-ray crystal structure of the *trp* repressor–operator complex. The monomers of the *trp* repressor dimer are coloured yellow and green. Water molecules are represented by blue spheres. **(b)** Representation of the X-ray crystal structure of the MetJ–metbox complex. The monomers of the MetJ protein dimer are coloured yellow and green. Water molecules are represented by blue spheres.

biomolecular interactions. At present, there is only limited information on the thermodynamics of many of the systems discussed above, and much work remains to be conducted if we are to understand the underlying forces that govern these interactions. One goal of these studies is to be able to predict the thermodynamic components of an interaction from structural detail alone, and *vice versa*.

Acknowledgements

We dedicate this review to Professor Julian M. Sturtevant for the inspiring example he has set us in our scientific careers.

References

1. Kuntz I.D. & Kauzmann, W. (1974). Hydration of proteins and polypeptides. *Adv. Protein Chem.* **28**, 239–345.
2. Tanford, C. (1980). *The Hydrophobic Effect.* Wiley-Interscience, New York.
3. Edsall, J.T. & McKenzie, H.A. (1983). Water and proteins. II. The location and dynamics of water in protein systems and its relation to their stability and properties. *Adv. Biophys.* **16**, 53–183.
4. Connelly, P.R. (1994). Acquisition and use of calorimetric data for the prediction of the thermodynamics of ligand-binding and folding reactions of proteins. *Curr. Opin. Biotechnol.* **5**, 381–388.
5. Sturtevant, J.M. (1977). Heat capacity and entropy changes in processes involving proteins. *Proc. Natl. Acad. Sci. USA.* **74**, 2236–2240.
6. Baldwin, R.L. (1986). Temperature dependence of the hydrophobic interaction in protein folding. *Proc. Natl. Acad. Sci. USA.* **83**, 8069–8072.
7. Livingstone, J.R., Spolar, R.S. & Record, M.T. (1991). The contribution to the thermodynamics of protein folding from reduction in water-accessible nonpolar surface area. *Biochemistry* **30**, 4237–4244.
8. Murphy, K.P. & Gill, S.J. (1991). Solid model compounds and the thermodynamics of protein unfolding. *J. Mol. Biol.* **222**, 699–709.
9. Ha, J.-H., Spolar, R.S. & Record, M.T. (1989). Role of the hydrophobic effect in stability of site-specific protein–DNA complexes. *J. Mol. Biol.* **209**, 801–816.
10. Spolar, R. & Record, M.T. (1994). Coupling of local folding to site-specific binding of proteins to DNA. *Science* **263**, 777–783.
11. Naghibi, H., Tamura, A., & Sturtevant, J.M. (1995). Significant discrepancies between the van't Hoff and calorimetric enthalpies. *Proc. Natl. Acad. Sci. USA.* **92**, 5597–5599.
12. Wyman, J. & Gill, S.J. (1990) *Binding and Linkage: Functional Chemistry of Biological Macromolecules.* University Science Books, Sausalito, CA, USA.
13. Wiseman, T., Williston, S., Brandts, J.F. & Lin, L.N. (1989). Rapid measurement of binding constants and heats of binding using a new titration calorimeter. *Anal. Biochem.* **179**, 131–137.
14. Freire, E., Mayorga, O.L. & Straume, M. (1990). Isothermal titration calorimetry. *Anal. Chemistry* **62**, 950–954.
15. Connelly, P.R., Varadarajan, R., Sturtevant, J.M. & Richards, F.M. (1990). Thermodynamics of protein–peptide interactions in the ribonuclease S system studied by titration calorimetry. *Biochemistry* **29**, 6108–6114.
16. Varadarajan, R., Connelly, P.R., Sturtevant, J.M. & Richards, F.M. (1992). Heat capacity changes for protein–peptide interactions in the ribonuclease S system. *Biochemistry* **31**, 1421–1426.
17. Thomson, J., Ratnaparkhi, G.S., Varadarajan, R., Sturtevant, J.M. & Richards, F.M. (1994). Thermdynamic and structural consequences of changing a sulfur atom to a methylene group in the M13Nle mutation of ribonuclease S. *Biochemistry* **33**, 8587–8593.
18. Lu, M., Guo, Q., Marky, L.A., Seeman, N.C. & Kallenbach, N.R. (1992). Thermodynamics of DNA branching. *J. Mol. Biol.* **223**, 781–789.
19. Ladbury, J.E., Sturtevant, J.M. & Leontis, N.B. (1994). The thermodynamics of formation of a three-strand, DNA three-way junction complex. *Biochemistry* **33**, 6828–6833.
20. Kochoyan, M., & Leroy, J.L. (1995) Hydration and solution structure of nucleic acids. *Curr. Opin. Struct. Biol.* **5**, 329–333.
21. Haq, I., Lincoln, P., Suh, D., Norden, B., Chowdhry, B.Z. & Chaires, J.B. (1995). Interaction of Δ- and Λ-$[Ru(phen)_2DPPZ]^{2+}$ with DNA: a calorimetric and equilibrium binding study. *J. Am. Chem. Soc.* **117**, 4788–4796.
22. Hopkins, H.P., Fumero, J., & Wilson, W.D. (1990). Temperature dependence of enthalpy change for ethidium and propidium binding to DNA: effect of the alkylamine chain. *Biopolymers* **29**, 449–459.
23. Chaires, J.B., Priebe, W., Graves, D.E. & Burke, T.G. (1993). Dissection of the free energy of anthracycline antibiotic binding to DNA: electrostatic contributions. *J. Am. Chem. Soc.* **115**, 5360–5364.
24. Lemmon, M.A. & Ladbury, J.E. (1994). Thermodynamic studies of tyrosyl-phosphopeptide binding to the SH2 domain of $p56^{lck}$. *Biochemistry* **33**, 5070–5076.
25. Lemmon, M.A., Ladbury, J.E., Mandiyan, V., Zhou, M. & Schlessinger, J. (1994). Independent binding of peptide ligands to the SH2 and SH3

domains of Grb2. *J. Biol. Chem.* **269**, 31653–31658.
26. Ladbury, J.E., Lemmon, M.A., Zhou, M. Green, J., Botfield, M. & Schlessinger, J. (1995). Measurement of the binding of tyrosyl phosphopeptides to SH2 domains: a reappraisal. *Proc. Natl. Acad. Sci. USA.* **92**, 3199–3203.
27. Ladbury, J.E., Hennsman, M., Panayotou, G. & Campbell, I.D.C. (1996). Alternative modes of tyrosyl phosphopeptide binding to a Src family SH2 domain: implications for regulation of tyrosine kinase activity. *Biochemistry* **35**, 11062–11069.
28. Ladbury, J.E. (1995). Counting the calories to stay in the groove. *Structure* **3**, 635–639.
29. Bains, G. & Freire, E. (1991). Calorimetric determination of cooperative interaction in high affinity binding processes. *Anal. Biochem.* **192**, 203–206.
30. Sigurskjold, B.W., Berland, C.R., & Svensson, B. (1994). Thermodynamics of inhibitor binding to the catalytic site of glucoamylase from *Aspergillus niger* determined by displacement isothermal titration calorimetry. *Biochemistry* **33**, 10191–10199.
31. Lohman, T.M., & Mascotti, D.P. (1992). Thermodynamics of ligand–nucleic acid interactions. *Methods Enzymol.* **212**, 424–458.
32. Ladbury, J.E., Wright, J.G., Sturtevant, J.M. & Sigler, P.B. (1994). A thermodynamic study of the *trp* repressor–operator interaction. *J. Mol. Biol.* **238**, 669–681.
33. Hyre, D.E. & Spicer, L.D. (1995). Thermodynamic evaluation of binding interactions in the methionine repressor system of *Escherichia coli* using isothermal titration calorimetry. *Biochemistry* **34**, 3212–3221.
34. Cunningham, B.C., Ultsch, M., deVos, A.M., Mulkerrin, M.G., Glauser, K.R. & Wells, J.A. (1991). Dimerization of the extracellular domain of the human growth hormone receptor by a single hormone molecule. *Science* **254**, 821–825.
35. Spivak-Kroizman, T., *et al.*, & Lax, I. (1994). Heparin-induced oligomerization of FGF molecules is responsible for FGF receptor dimerization, activation, and cell proliferation. *Cell* **79**, 1015–1024.
36. Gomez, J. & Freire, E. (1995). Thermodynamic mapping of the inhibitor site of the aspartic protease endothiapepsin. *J. Mol .Biol.* **252**, 337–350.
37. Connelly, P.R. & Thomson, J.A. (1992). Heat capacity changes and hydrophobic interactions in the binding of FK506 and rapamycin to the FK506 binding protein. *Proc. Natl. Acad. Sci. USA.* **89**, 4781–4785.
38. Morton, C.J. & Ladbury, J.E. (1996). Water mediated protein–DNA interactions: the relationship of thermodynamics to structural detail. *Protein Sci.*, in press.